Journal of Advanced Sport Technology
DOI: 10.22098/jast.2025.18618.1444
Received: 21 Oct 2025 Accepted: 24 Nov 2025

ORIGINAL ARTICLE *Open Access*

Multifractal Complexity Analysis of Electroencephalography (EEG) Signals and Kinematic Dynamics During Walking

Rouhollah Basatnia, Mehrdad Anbarian *[2] & Afshin Montakhab [3]

1. Ph.D Candidate, Department of Sports Biomechanics, Faculty of Physical Education, Bu-Ali Sina University, Hamedan, Iran.
2. Associate Professor, Department of Sports Biomechanics, Faculty of Physical Education, Bu-Ali Sina University, Hamedan, Iran.
3. Professor, Department of Physics, Faculty of Sciences, Shiraz University, Shiraz, Iran.

Correspondence: anbarrian@basu.ac.ir

ABSTRACT

Background: Walking, as a complex motor activity, requires precise coordination within the neuromuscular system. This study aimed to analyze the multiscale complexity of electroencephalography (EEG) signals and kinematic data during walking to investigate brain-lower limb interactions.

Methods: Thirteen male participants walked on a treadmill under controlled conditions, during which EEG signals and kinematic data were recorded. Multifractal complexity analysis using the multifractal detrended fluctuation analysis (MF-DFA) method was applied to the data to extract the Hurst exponent as a complexity index for dynamic features of movements in displacement dimensions along three axes (X, Y, Z) and cortical activity in motor brain regions (C3 and C4) during walking.

Results: Results indicated that the generalized Hurst exponent H(q) in the C3 and C4 regions was similar and exhibited a significant positive correlation with the same parameter in the dynamics of the contralateral limb, supporting the principle of interhemispheric control. Segmental analysis of the thigh, shank, and foot revealed substantial dynamic symmetry between the right and left sides. The multifractal patterns of the segments demonstrated significant differences, with the highest H(q) in the shank and the lowest in the thigh. Strong intra-system coordination among segments suggests an integrated organization in motor control.

Conclusions: These findings confirm neuromuscular symmetry and coordination, provide utility for assessing motor disorders and designing rehabilitation protocols, and underscore the importance of multiscale analysis in elucidating complex brain-body interactions, with potential applications in neuroscience, biomechanics, and rehabilitation research.

KEYWORDS: Walking, EEG signals, kinematic data, multifractal analysis, Hurst exponent

How to cite: Anbarian, M., Basatnia, R. Multifractal Complexity Analysis of Electroencephalography (EEG) Signals and Kinematic Dynamics During Walking. *Journal of Advanced Sport Technology*, 2026; 10(2): 13-24. doi: 10.22098/jast.2025.18618.1444

Introduction

Analysis of electroencephalography (EEG) signal complexity can reveal neural processing patterns associated with motor planning and execution, while kinematic data provide insights into the coordination, symmetry, and dynamics of lower limb movements [١]. Studies have demonstrated that alterations in gait patterns, such as reduced stability or step asymmetry, can be identified under the influence of neurological disorders like Parkinson's disease or stroke. For example, simultaneous EEG and kinematic analysis in patients with Parkinson's disease has more precisely delineated motor deficits and compensatory mechanisms[٢] . However, most prior investigations have focused on separate or single-scale analyses of these data, with limited attention to concurrent and multiscale examinations of brain-body interactions during walking [٣]. Biological signals such as EEG and kinematic data often exhibit nonlinear and complex behaviors that traditional linear analysis methods may not fully capture [٤]. Multifractal analysis, designed to probe signals exhibiting multifractal scaling behaviors, provides a robust tool for elucidating the complexity and variability of these signals [٥]. This approach, employing indices such as the Hurst exponent and the multifractal spectrum, enables the examination of signal dynamic features across multiple scales. Detrending in time series analysis entails the removal of the trend or overall drift (Trend) from the data to uncover the intrinsic fluctuations of the time series, free from the effects of gradual changes or long-term trends. For instance, in gait kinematic studies, it involves eliminating the shared and trending components of kinematic data curves (across various walking cycles of an individual) and conducting analytical processing on the unique, non-shared portions of each cycle relative to the others. The primary objective of detrending is to facilitate a more accurate analysis of fluctuations and stochastic behaviors in the data [٦].

The multifractal detrended fluctuation analysis (MF-DFA) method serves as a powerful tool for investigating nonlinear and self-similar dynamics in biological data, enabling the analysis of complexity patterns across various temporal scales [٧]. By extracting the Hurst exponent and identifying multiscale features, this method aids in understanding alterations in neuromuscular control and responses to interventions [٨]. Clinical applications of MF-DFA encompass early detection of motor disorders, evaluation of rehabilitation program efficacy, and design of intelligent prostheses that synchronize with natural gait patterns [٩]. In recent years, this analysis has been extensively employed to study EEG signals in cognitive and motor tasks. For instance, researchers utilized detrended multifractal analysis to classify cognitive tasks based on EEG signals, demonstrating its efficacy in extracting nonlinear signal features [١٠]. MF-DFA is specifically designed to identify self-similarity and multifractal structures in time series, determining whether the data exhibit similar or divergent behaviors across different scales and moments. It has been shown that multifractal analysis of EEG correlates with cognitive test scores in mild cognitive impairment [١١]. Additionally, a group of researchers, employing multifractal analysis and entropy, revealed spatial organization in local functional connectivity of resting-state

EEG [١٢]. Another group applied multifractal analysis to examine EEG during actual and imagined movements [٣١]. In the realm of human locomotion, multifractal analysis has been used to study the complexity of gait patterns, as it can detect structured or random characteristics in the residual data following the removal of common trends. Previously, researchers proposed a multifractal dynamic model for human walking that indicates the presence of multifractal features in stride interval time series [١٤]. More recently, investigators applied multiscale multifractal analysis to human movements during cognitive tasks, providing insights into motor coordination [١٥]. Despite these advancements, few studies have concurrently performed multifractal analysis on EEG signals and kinematic data during walking. Integrating these two data types can offer a more comprehensive understanding of neural control in gait. Datasets combining kinematics, kinetics, and EMG data in walking provide valuable resources for this purpose [١٦]. This study aims to address the existing research gap by employing the MF-DFA method to analyze the multiscale complexity of EEG signals and kinematic data during the walking process. We seek to examine the nonlinear relationships between brain activity (focusing on the motor cortex) and motor dynamics (emphasizing limb displacements during walking) across various temporal scales. The intention is to analyze the residual data in each gait cycle—after removing the shared brain and motion components across cycles—to elucidate their self-similarity features. The results of this research can establish a framework for natural walking behavior in both neural and biomechanical dimensions, with applications in diagnosing neurological disorders, designing advanced robotic systems, and enhancing rehabilitation programs for patients with motor impairments.

Material and Methods

Procedure: Participants walked on a treadmill under controlled conditions with no incline, and the experimental protocol consisted of two primary stages. Initially, participants underwent training to familiarize themselves with the apparatus, its operation, and treadmill locomotion, thereby enhancing their comfort level. Subsequently, during the speed adjustment phase, participants first walked for 1 minute at a fixed speed, followed by 1 minute at a speed approaching the transition threshold from walking to running. These stages were designed to determine the preferred walking speed and facilitate participant adaptation to treadmill conditions. In the main phase, participants performed 1 minute of walking on the treadmill at their preferred speed. EEG data was captred using a LIV EEG system with active electrodes along motor cortex (C3 and C4 regions) as showed on Fig. 1 using conventional 10-20 electrode placement system.

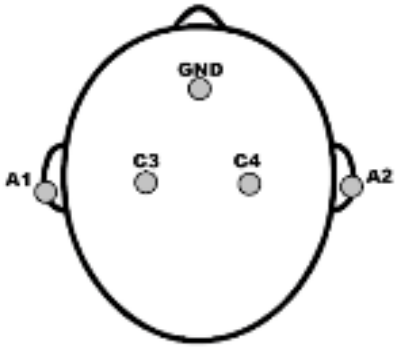

Figure 1: Electrode placement based on 10-20 system

Data Processing: The recorded EEG signals underwent preprocessing in MATLAB software using the EEGLab toolbox to remove artifacts and noise, encompassing three main stages. In the first stage, a finite impulse response (FIR) filter with a frequency band of 1–30 Hz was applied to eliminate high- and low-frequency noise. Subsequently, in the second stage, independent component analysis (ICA) was employed to identify and remove potential artifacts; this method facilitated the detection and elimination of non-essential components, such as motion-induced vibrations affecting electrode recordings. Following artifact identification, non-essential components were removed, and signals were labeled based on events recorded in MATLAB software, thereby enhancing the accuracy of signal analysis.

For kinematic data processing, the x-component displacement of heel markers for each foot (as per Figure 2)—due to the curve's single extremum—was initially utilized to extract gait pattern recognition and timing for left and right steps. Data analysis was conducted using the SciPy and NumPy libraries in the Python programming environment, executed in two main stages. In the first stage, kinematic data were converted to CSV format, and marker displacement parameters in three dimensions were extracted. At this stage, based on the conventional marker averaging method, the positions of virtual distal and proximal markers for the thigh, shank, and foot segments were determined. Given that the Hurst exponent focuses on examining time series dynamics as an indicator of the complexity of the studied system's behavior, for simplicity, only the positions of virtual distal and proximal markers for the thigh, shank, and foot segments were selected as preferred time series for assessing walking motion complexity. Then, in the second stage, multifractal detrended fluctuation analysis (MF-DFA) was performed on the data. This analysis, utilizing standard methods, was dedicated to extracting fluctuations and motion characteristics and included steps such as constructing the time series profile, dividing data into equal segments, fitting and detrending, calculating fluctuations, and extracting H(q). The steps of this analysis are as follows: Based on the DFA and MFDFA methods proposed by previous studies]6[, all data were normalized as time series to achieve zero mean and unit variance, where $\bar{x}$ is the mean of the time series and σ_x is the standard deviation of the time series.

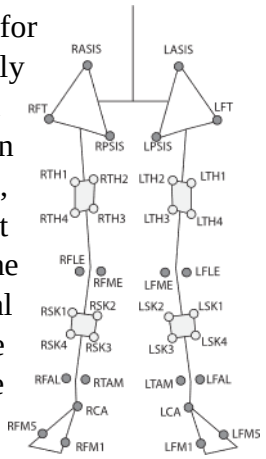

Figure 2;The markerset that used in lower extremity

$$(١) \qquad xk' = \frac{x_k - \bar{x}}{\sigma_x}$$

To elucidate the cumulative variations in the data, the cumulative profile $Y(i)$ was computed, representing the cumulative sum of deviations of the time series from its mean:

$$(٢) Y(i) = \sum_{k=1}^{i} (x_k - \bar{x})$$

The time series data were divided into non-overlapping segments for each scale τ. These segments corresponded to complete gait cycles for the right foot markers in the right foot cycles and for the left foot markers in the left foot cycles. These cycles were extracted from the x-component displacement of the heel marker for each foot. This approach was chosen due to the clear identification of extremum points (maxima and minima) in the gait cycle within this marker's

component, which repeats solely across walking cycles. Figure 3 delineates the segmentation points of the time series for the left and right gait cycles.

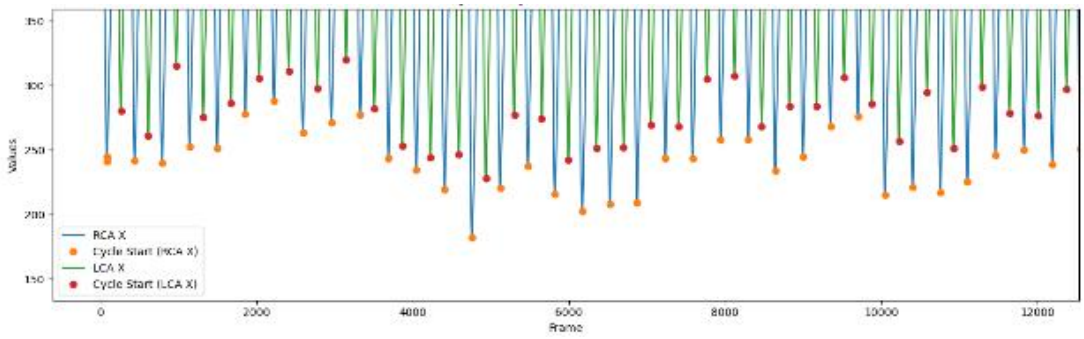

Figure 3: Boundaries of each step based on the x component of the right heel (RCA) and the left heel (LCA) markers

The profile $Y(i)$ was partitioned into N_s segments of length s, where s denotes various temporal scales, typically selected as powers of 2. To ensure full data coverage, segmentation from the end was also performed using the reversed data ($s = 2, 4, 8, 16, ...$). To remove local trends, a polynomial of degree m was fitted within each segment $v\backslash nu$, where 1≤v≤N_s:

$$(٣)Pv, m(i) == c_0 + c_1 i + c_2 i^2 + \cdots + c_m i^m$$

The detrended signal was then computed by subtracting this polynomial from the profile data:

$$(٤)Y_{detrended,v}(i) = Y(i) - P_{v,m}(i)$$

The fluctuation function $Fq(s)$ for each segment was calculated, where q is the order parameter:

$$(٥)F_q(s) = \left(\frac{1}{2N_s}\sum_{v=1}^{2N_s}\left[\frac{1}{s}\sum_{i=1}^{s}\left(Y_{\text{detrended},v}(i)\right)^2\right]^{q/2}\right)^{1/q}$$

For $q = 0$, the following limit was employed:

$$(٦)F_0(s) = \exp\left(\frac{1}{2N_s}\sum_{v=1}^{2N_s}\ln\left[\frac{1}{s}\sum_{i=1}^{s}\left(Y_{\text{detrended},v}(i)\right)^2\right]\right)$$

For each q, the following logarithmic relation was examined:

$$(٧)l\,n\,F\,q(s) \sim h(q)\ln s$$

The slope of the fitted line on the plot of $\log F_q(s)$versus $\log s$ yields the q-order Hurst exponent $h(q)$. The Hurst exponents $h(q)$were computed over a wide range of q, such as from -5 to 5. These values highlighted distinct data characteristics: for $q > 0$, the dependence of larger fluctuations was examined, whereas for $q < 0$, emphasis was placed on smaller fluctuations.

Statistical Analyses: Relationships between the complexity of EEG signals and kinematic data were examined using descriptive statistics (mean, median, standard deviation, and range) for the

Hurst exponent of each time series. Associations between EEG signal complexity and kinematic data were assessed via Pearson correlation coefficient (significance level: $p < 0.05$). One-way analysis of variance (ANOVA) was conducted to compare Hurst exponents across segments (thigh, shank, foot) and brain regions (C3, C4). Analyses were performed in Python using the SciPy library. These computations provided a clear depiction of data distribution and primary characteristics among participants. Appropriate q values (0, 2) were selected based on the research context [6]. Data normality was evaluated using the Shapiro-Wilk test, and accordingly, the mean served as the central tendency measure, the median for assessing symmetric distributions, and the standard deviation for quantifying data dispersion, thereby enabling a more precise examination of the collected data features. Additionally, the range of variations aided in identifying potential differences across participants. Subsequently, correlational and comparative analyses were employed to test the research hypotheses. This two-stage approach not only facilitated a rigorous evaluation of group-level data but also yielded key insights into the interrelationships between brain signal complexity and kinematic walking features as derived from MF-DFA.

Results

In total, the displacement data of the virtual markers for the right and left thigh, shank, and foot segments in the three axes (X, Y, Z), along with cortical activity in the left and right motor regions, were analyzed using the multifractal detrended fluctuation analysis (MF-DFA) method (Figure 4). The Hurst exponent data—as one of the most important complexity indices in this method—for the entire group are presented in Tables 1 and 2, along with the results of normality testing (Shapiro-Wilk) for the data.

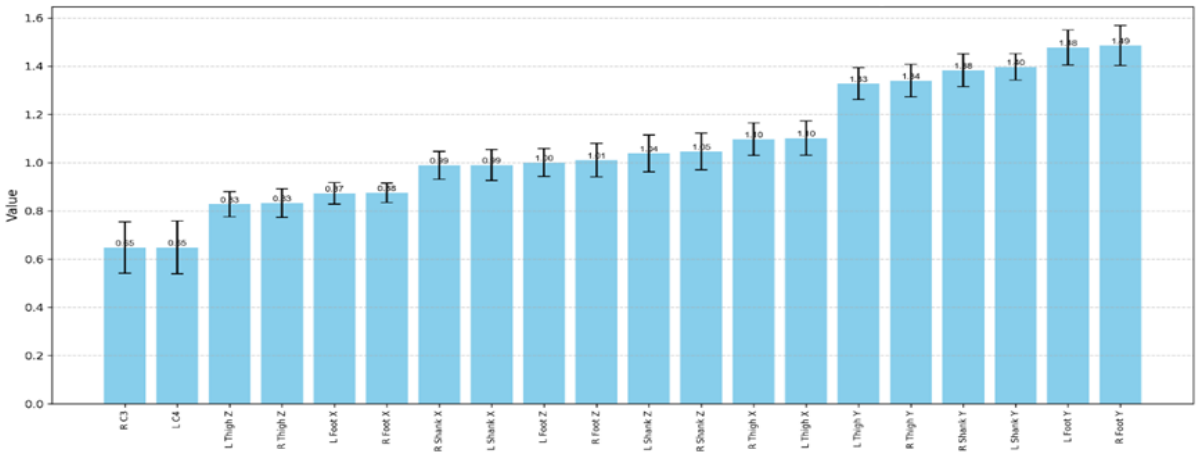

Figure 4: Distribution of the mean of the Hurst function among the statistical sample

Table 1: Normality tests of Hurst exponent mean in brain and lower extremities of subjects (Shapiro-Wilk)

Signal	W	p-value
C4	0.89	0.10
LEFT FOOT X Mean	0.96	0.83
LEFT FOOT Y Mean	0.96	0.79
LEFT FOOT Z Mean	0.97	0.97
LEFT SHANK X Mean	0.85	0.03
LEFT SHANK Y Mean	0.89	0.12
LEFT SHANK Z Mean	0.95	0.65
LEFT TIGHT X Mean	0.94	0.58
LEFT TIGHT Y Mean	0.90	0.17
LEFT TIGHT Z Mean	0.97	0.89
C3	0.90	0.14
RIGHT FOOT X Mean	0.97	0.94
RIGHT FOOT Y Mean	0.82	0.01
RIGHT FOOT Z Mean	0.96	0.86
RIGHT SHANKX Mean	0.94	0.46
RIGHT SHANKY Mean	0.97	0.91
RIGHT SHANKZ Mean	0.93	0.42
RIGHT TIGHTX Mean	0.86	0.03
RIGHT TIGHTY Mean	0.93	0.35
RIGHT TIGHTZ Mean	0.98	0.99

Table 2: Descriptive statistics of Hurst exponent in the brain and displacement of the left and right markers

Signal	mean	std	count	min	max
C4	0/64	0/10	13	0/42	0/85
LEFT FOOT X Mean	0/87	0/04	13	0/79	0/97
LEFT FOOT Y Mean	1/47	0/07	13	1/35	1/60
LEFT FOOT Z Mean	1/00	0/05	13	0/88	1/09
LEFT SHANK X Mean	0/99	0/06	13	0/92	1/13
LEFT SHANK Y Mean	1/39	0/05	13	1/30	1/459
LEFT SHANK Z Mean	1/038	0/07	13	0/90	1/14
LEFT TIGHT X Mean	1/10	0/07	13	0/97	1/26
LEFT TIGHT Y Mean	1/32	0/06	13	1/21	1/40
LEFT TIGHT Z Mean	0/82	0/05	13	0/72	0/92
C3	0/64	0/10	13	0/42	0/83
RIGHT FOOTX Mean	0/87	0/04	13	0/80	0/95
RIGHT FOOTY Mean	1/48	0/08	13	1/30	1/58
RIGHT FOOTZ Mean	1/01	0/06	13	0/86	1/13
RIGHT SHANKX Mean	0/98	0/05	13	0/90	1/10
RIGHT SHANKY Mean	1/38	0/06	13	1/24	1/48
RIGHT SHANKZ Mean	1/04	0/07	13	0/91	1/14
RIGHT TIGHTX Mean	1/09	0/06	13	1/00	1/27
RIGHT TIGHTY Mean	1/33	0/06	13	1/18	1/44
RIGHT TIGHTZ Mean	0/83	0/05	13	0/71	0/93

The generalized Hurst exponent H(q) values in the primary motor regions revealed that electroencephalography (EEG) activity in the C3 region (right hemisphere) and C4 region (left hemisphere) exhibited a similar pattern. The mean H(q) in C3 was 0.648 ± 0.107, and in C4, it was 0.649 ± 0.110, with no statistically significant difference ($t(24) = 0.021$, $p = 0.984$). The range of variations in C3 spanned from 0.420 to 0.839, and in C4, from 0.423 to 0.854. Correlation analysis indicated that activity in the C3 region exhibited a significant positive correlation with the motor dynamics of the left foot ($r = 0.62$, $p = 0.021$), and activity in the C4 region with the motor dynamics of the right foot ($r = 0.54$, $p = 0.048$). The present study, through examination of the generalized Hurst exponent values in the lower limbs, unveiled an intriguing pattern of functional symmetry. Statistical analyses, including paired t-tests and effect size calculations, demonstrated no statistically significant differences between right- and left-side body performance across any of the examined segments (thigh, shank, and foot, $p > 0.05$).

The mean difference between sides was only 0.008 ± 0.023, which is considered clinically negligible (95% confidence interval: -0.026 to 0.042), and the calculated effect size (d = 0.07) was trivial. Analysis of the left-side segments revealed significant differences in multifractal activity patterns across various lower limb sections ($F(2, 36) = 58.37$, $p < 0.001$). In other words, the self-similarity of these data varied across these sections. Specifically, the shank exhibited the highest mean H(q) of 1.142 ± 0.065, while the thigh showed the lowest at 1.086 ± 0.063. Tukey's post-hoc test confirmed these differences as statistically significant ($p < 0.05$). In the axial analysis, the Y-axis recorded the highest mean H(q) of 1.401 ± 0.064, and the Z-axis the lowest at 0.956 ± 0.062. These findings were fully consistent with those on the right side. One-way ANOVA indicated significant differences between segments ($F(2, 36) = 62.18$, $p < 0.001$). Similar to the left side, the shank displayed the highest mean H(q) of 1.140 ± 0.067, and the thigh the lowest at 1.090 ± 0.064. The axial pattern on the right side mirrored that of the left, with the Y-axis showing the highest mean value (1.403 ± 0.072), followed by the X-axis (0.987 ± 0.055), and finally the Z-axis (0.963 ± 0.068). This bilateral consistency underscores a systematic and coordinated organization in neuromuscular motor control. Furthermore, intra-side correlation analyses unveiled a notable pattern of functional coordination. Across both sides of the body, correlations between segments were very strong and significant ($r > 0.75$, $p < 0.001$). These findings suggest that, following the removal of common trends in these motor and neural data (distinct from the analysis of primary trends in biomechanics), the residual non-common trends also adhere to an underlying order and stability. Evidently, the neuromuscular system employs an integrated pattern for motion control. Notably, the high correlation between the shank and foot (left side: $r = 0.82$; right side: $r = 0.79$) may highlight the critical role of this linkage in postural control and gait.

The findings presented in Table 3 indicate that the EEG activity pattern in the motor regions is symmetric and supports contralateral motor control. Furthermore, strong intra-system coordination exists between various sections of these regions ($p < 0.05$).

Table 3: EEG results and correlation with contralateral limb movement dynamics

Region/Segment	Mean H(q) ± SD	Range	Correlation with Contralateral Limb Motor Dynamics
C3 - Right Hemisphere	0.648 ± 0.107	0.420–0.839	r = 0.62* (with left foot)
C4 - Left Hemisphere	0.649 ± 0.110	0.423–0.854	r = 0.54* (with right foot)

Discussion

This study utilized multifractal detrended fluctuation analysis (MF-DFA) to examine the dynamic complexity of electroencephalography (EEG) signals and kinematic data during walking in healthy young adults. The findings offer valuable insights into brain-body interactions underlying motor control, underscoring the symmetry of cerebral and locomotor activity in healthy individuals. In this section, the key results are discussed and interpreted in relation to the existing literature, with a focus on the primary dimensions highlighted.

Motor Brain Regions: The findings of this study revealed that the Hurst exponent H(q) in the C3 and C4 regions was highly similar. The mean H(q) for C3 was 0.648 and for C4, 0.649 ($p = 0.41$), indicating equivalent dynamic complexity in neural activity across both hemispheres. This symmetry aligns with prior studies employing nonlinear analyses, such as the Hurst exponent, to investigate EEG. For instance, a study utilizing the Hurst exponent to extract nonlinear EEG features [17] demonstrated that EEG signal complexity can be comparable under varying conditions. Additionally, another investigation reported high coordination between left and right motor brain regions during voluntary muscle contractions, supporting functional interhemispheric coordination [18]. Furthermore, a study examining EEG differences in left- and right-hand motor imagery found that subtle differences between hemispheric EEG signals could be induced through training, yet overall symmetry in brain activity was observed [19]. These results affirm that, in healthy individuals, motor control-related brain activities in both hemispheres operate symmetrically; however, external factors such as noise or volume conduction effects may influence Hurst exponent estimation [20], highlighting the need for more refined analyses in future studies.

Lower Limbs: The results of this study indicated that the dynamic complexity of thigh, shank, and foot movements was highly similar across both sides of the body, with minor differences in the lateral (Y) and vertical (Z) axes. For example, the mean H(q) for the Y-axis in the left shank (1.397) was slightly higher than in the right shank (1.383), and greater complexity was observed in the right foot along the Y and Z axes. This overall symmetry is consistent with gait studies in healthy individuals. A study applying fractal analysis to examine gait variability showed that gait patterns in healthy individuals are typically symmetric, with the Hurst exponent serving as an index for assessing gait adaptability [21]. Moreover, another research highlighted that gait complexity in healthy individuals reflects neuromuscular coordination [22]. However, in pathological conditions such as Parkinson's disease, gait asymmetry may increase [22], suggesting that the symmetry findings of this study are consistent with the existing literature for healthy populations. The minor differences observed in the Y and Z axes may relate to weight distribution or specific motion patterns, warranting further investigation under diverse locomotor conditions.

Right and Left Sides: The overall mean Hurst exponent for the right foot (1.118) and left foot (1.115) indicates general symmetry in the dynamic complexity of lower limb movements. This finding aligns with previous studies investigating gait symmetry in healthy individuals. One study demonstrated that step-to-step variability in walking is typically symmetric in healthy individuals but diminishes in Parkinson's disease [23]. Additionally, a study employing nonlinear analyses to examine gait dynamics confirmed that walking complexity in healthy individuals reflects high coordination within neural and muscular systems [24]. The symmetry observed in our findings suggests that, under normal conditions, both feet operate in a coordinated manner, consistent with the brain's symmetric control role in bilateral movements.

Comparison of Brain Activity and Foot Movements: A key finding of this study is the higher complexity of foot movements (mean $H(q) \approx 1.115–1.118$) compared to brain activity (mean $H(q) \approx 0.648–0.649$). This disparity may stem from the distinct natures of motor and neural signals. Foot movements are influenced by multiple factors, including balance, weight distribution, and neuromuscular coordination, which contribute to greater complexity. In contrast, brain activity, particularly in motor regions, primarily serves a regulatory function and may exhibit greater stability. A study examining the relationship between foot muscle activation and EEG during walking revealed that EEG and EMG signals in Parkinson's disease display nonlinear and scale-invariant behaviors [25], corroborating the elevated complexity of motor signals. Furthermore, an investigation of gait-related potentials indicated that EEG can reflect motor

patterns, though its complexity may be lower than that of motor signals [26]. Moreover, studies utilizing the Hurst exponent for EEG analysis in motor tasks have shown that EEG signals during motor imagery tasks exhibit moderate complexity [27,28], aligning with our results. Another study posited that integrating EEG with other methods can enhance understanding of brain-movement interactions [29].

Stability of Movements Across Axes: Kinematic data demonstrated that movement stability in the anterior-posterior axis (X) was substantially higher than in the lateral (Y) and vertical (Z) axes [30]. This observation is consistent with previous studies, which suggest that forward locomotion demands a superior level of control and stability to sustain propulsion and equilibrium. The reduced stability in the vertical axis may relate to ongoing adjustments to counter gravitational forces and maintain center-of-mass height [31]. Additionally, the progressive increase in Y-axis stability from proximal to distal segments may underscore the foot's role in upholding lateral balance [32].

The findings of this study align with the existing literature on the complexity analysis of EEG and motion signals, demonstrating symmetry in cerebral and locomotor activity among healthy individuals. The observed symmetry in the C3 and C4 regions, as well as in lower limb movements, is consistent with prior studies examining neuromuscular coordination in healthy populations [18,21]. The disparity in complexity between motor and neural signals may relate to their distinct roles in motor control and execution. Motor signals exhibit greater complexity due to involvement of mechanical and environmental factors, whereas neural signals display higher stability. These results hold potential applications in designing brain-computer interfaces (BCI) or rehabilitation programs for patients with motor disorders, such as Parkinson's disease [33]. For instance, multifractal analysis could facilitate early detection of neurodegenerative diseases or the development of intelligent prostheses that synchronize with natural gait patterns [34].

This study is subject to several limitations. The small sample size (13 participants, exclusively young males) may constrain the generalizability of the findings, particularly considering gender and age-related differences in gait [35]. Additionally, the experiments were conducted on a treadmill at controlled speeds, which may not fully capture the variability of overground walking in real-world environments. EEG analysis was confined to the C3 and C4 regions, and incorporating other areas, such as the premotor cortex or cerebellum, could provide a more comprehensive perspective. Moreover, noise and volume conduction effects may have influenced Hurst exponent estimates [20].

Future research could enhance generalizability by expanding the sample size to include females and diverse age groups, while investigating varied walking conditions (e.g., natural terrain or variable speeds). Analyzing additional brain regions and integrating multifractal methods with spectral analyses could yield deeper insights into the neural mechanisms of gait control. Furthermore, examining these patterns in patients with neurological disorders, such as Parkinson's disease or stroke, could bolster the clinical applicability of this approach.

Conclusion

This study, through multifractal analysis, unveiled the intricate interactions between cerebral activity and locomotor dynamics during walking. The symmetry in C3 and C4 activity, lower limb movements, and the elevated complexity of foot motions relative to neural signals affirm neuromuscular coordination in healthy individuals. These findings pave the way for clinical applications in diagnosis and rehabilitation, as well as future investigations into motor control.

Ethical Considerations:

Compliance with ethical guidelines

This study was conducted in accordance with the ethical standards outlined in the Declaration of Helsinki (1964, as revised in 2013). The research protocol was approved by the Medical Ethics Committee of Bu-Ali Sina University (Ethics Code: IR.BASU.REC.1402.019). All participants provided written informed consent prior to enrollment, and they were informed of their right to withdraw from the study at any time without any consequences. No identifying information was collected or stored, ensuring participant anonymity and data confidentiality.

Funding

This research received no specific grant from any funding agency in the public, commercial, or not-for-profit sectors. The study was supported by internal resources from the Department of Sports Biomechanics, Faculty of Physical Education, Bu-Ali Sina University. The funding body had no role in the design of the study, collection, analysis, and interpretation of data, or in writing the manuscript.

Conflict of Interest

The authors declare no conflict of interest.

Acknowledgment

The authors express their sincere gratitude to the participants for their voluntary involvement in this study. We also thank the technical staff at the Biomechanics Laboratory of Bu-Ali Sina University for their assistance in data collection and equipment setup. Special appreciation is extended to Dr. Afshin Montakhab, who provided valuable feedback on the statistical analyses during the preparation of this manuscript. All individuals mentioned here have granted permission for their acknowledgment. No professional writing services were utilized in the preparation of this article.

References

1. Busa MA, van Emmerik REA. Multiscale entropy: A tool for understanding the complexity of postural control. J Sport Health Sci 2016;5:44–51. DOI: 10.1016/j.jshs.2016.01.018
2. Shine JM, Matar E, Ward PB, Bolitho SJ, Pearson M, Naismith SL, et al. Differential Neural Activation Patterns in Patients with Parkinson's Disease and Freezing of Gait in Response to Concurrent Cognitive and Motor Load. PLoS One 2013;8:e52602. DOI: 10.1371/journal.pone.0052602
3. Stergiou N, Stergiou N, Decker LM, Decker LM. Human movement variability, nonlinear dynamics, and pathology: Is there a connection? Hum Mov Sci 2011. DOI: 10.1016/j.humov.2011.06.002
4. Zorick T, Mandelkern MA. Multifractal Detrended Fluctuation Analysis of Human EEG: Preliminary Investigation and Comparison with the Wavelet Transform Modulus Maxima Technique. PLoS One 2013;8:e68360. DOI: 10.1371/journal.pone.0068360
5. Racz FS, Stylianou O, Mukli P, Eke A. Multifractal and entropy analysis of resting-state electroencephalography reveals spatial organization in local dynamic functional connectivity. Sci Rep 2019;9. DOI: 10.1038/s41598-019-49726-5

6. Ihlen EAF. Introduction to multifractal detrended fluctuation analysis in Matlab. Front Physiol 2012;3 JUN:23948. DOI: 10.3389/fphys.2012.00141
7. Delignières D, Torre K, Bernard PL. Transition from Persistent to Anti-Persistent Correlations in Postural Sway Indicates Velocity-Based Control. PLoS Comput Biol 2011;7:e1001089. DOI: 10.1371/journal.pcbi.1001089
8. Goldberger AL, Amaral LAN, Hausdorff JM, Ivanov PC, Peng CK, Stanley HE. Fractal dynamics in physiology: Alterations with disease and aging. Proc Natl Acad Sci U S A 2002;99:2466. DOI: 10.1073/pnas.012579499
9. Gaurav G, Anand RS, Kumar V. EEG based cognitive task classification using multifractal detrended fluctuation analysis. Cogn Neurodyn 2021;15:999–1013. DOI: 10.1007/s11571-021-09684-z
10. Zorick T, Landers J, Leuchter A, Mandelkern MA. EEG multifractal analysis correlates with cognitive testing scores and clinical staging in mild cognitive impairment. Journal of Clinical Neuroscience 2020;76:195–200. DOI: 10.1016/j.jocn.2020.04.003
11. Racz FS, Stylianou O, Mukli P, Eke A. Multifractal and entropy analysis of resting-state electroencephalography reveals spatial organization in local dynamic functional connectivity. Sci Rep 2019;9. DOI: 10.1038/s41598-019-49726-5
12. Pavlov AN, Maksimenko VA, Runnova AE, Khramova M V., Pisarchik AN. Multifractal analysis of real and imaginary movements: EEG study 2018;10717:35. DOI: 10.1117/12.2311482
13. West BJ, Scafetta N. A Multifractal Dynamical Model of Human Gait. Fractals in Biology and Medicine 2005:131–40. DOI: 10.1007/3-7643-7412-8_12
14. Faini A, Arsac LM, Deschodt-Arsac V, Castiglioni P. Multifractal Multiscale Analysis of Human Movements during Cognitive Tasks. Entropy 2024;26. DOI: 10.3390/E26020148
15. Lencioni T, Carpinella I, Rabuffetti M, Marzegan A, Ferrarin M. Human kinematic, kinetic and EMG data during different walking and stair ascending and descending tasks. Sci Data 2019;6:1–10. DOI: 10.1038/S41597-019-0323-z
16. Geng S, Zhou W, Yuan Q, Cai D, Zeng Y. EEG non-linear feature extraction using correlation dimension and Hurst exponent. Neurol Res 2011;33:908–12. DOI: 10.1179/1743132811Y.0000000041
17. Abdul-Latif AA, Cosic I, Kumar DK, Polus B, Pah N, Djuwari D. EEG coherence changes between right and left motor cortical areas during voluntary muscular contraction. Australas Phys Eng Sci Med 2004;27:11–5. DOI: 10.1007/BF03178882
18. Neuper C, Schlögl A, Pfurtscheller G. Enhancement of left-right sensorimotor EEG differences during feedback- regulated motor imagery. Journal of Clinical Neurophysiology 1999;16:373–82. DOI: 10.1097/00004691-199907000-00010
19. Blythe DAJ, Haufe S, Müller KR, Nikulin V V. The effect of linear mixing in the EEG on Hurst exponent estimation. Neuroimage 2014;99:377–87. DOI: 10.1016/J.NEUROIMAGE.2014.05.041
20. Phinyomark A, Larracy R, Scheme E. Fractal Analysis of Human Gait Variability via Stride Interval Time Series. Front Physiol 2020;11:333. DOI: 10.3389/FPHYS.2020.00333
21. Warlop T, Detrembleur C, Bollens B, Stoquart G, Crevecoeur F, Jeanjean A, et al. Degradation of gait autocorrelation as precocious marker of fall risk in Parkinson's disease. Ann Phys Rehabil Med 2015;58:e71. DOI: 10.1016/J.REHAB.2015.07.175
22. Hausdorff JM. Gait dynamics in Parkinson's disease: Common and distinct behavior among stride length, gait variability, and fractal-like scaling. Chaos 2009;19:026113. DOI: 10.1063/1.3147408
23. Decker LM, Cignetti F, Stergiou N. Complexity and human gait. Revista Andaluza de Medicina del Deporte. 2010;3(1):2-12. https://digitalcommons.unomaha.edu/biomechanicsarticles/91

24. Günther M, Bartsch RP, Miron-Shahar Y, Hassin-Baer S, Inzelberg R, Kurths J, et al. Coupling between leg muscle activation and EEG during normal walking, intentional stops, and freezing of gait in Parkinson's disease. Front Physiol 2019;10:870. DOI: 10.3389/FPHYS.2019.00870
25. Maidan I, Patashov D, Shustak S, Fahoum F, Gazit E, Shapiro B, et al. A new approach to quantifying the EEG during walking: Initial evidence of gait related potentials and their changes with aging and dual tasking. Exp Gerontol 2019;126. DOI: 10.1016/J.EXGER.2019.110709
26. Aldea R, Tarniceriu D. Estimating the hurst exponent in motor imagery-based brain computer interface. 2013 7th Conference on Speech Technology and Human - Computer Dialogue, SpeD 2013 2013. DOI: 10.1109/SPED.2013.6682656
27. Gupta A, Kumar D, Chakraborti A. Hurst Exponent as a New Ingredient to Parametric Feature Set for Mental Task Classification. Advances in Intelligent Systems and Computing 2018;701:129–37. DOI: 10.1007/978-981-10-7563-6_14
28. Hallett M, DelRosso LM, Elble R, Ferri R, Horak FB, Lehericy S, et al. Evaluation of movement and brain activity. Clinical Neurophysiology 2021;132:2608–38. DOI: 10.1016/J.CLINPH.2021.04.023
29. Phinyomark A, Larracy R, Scheme E. Fractal Analysis of Human Gait Variability via Stride Interval Time Series. Front Physiol 2020;11:333. DOI: 10.3389/FPHYS.2020.00333
30. Tesio L, Rota V. The Motion of Body Center of Mass During Walking: A Review Oriented to Clinical Applications. Front Neurol 2019;10. DOI: 10.3389/FNEUR.2019.00999
31. Ji Q, Qian Z, Ren L, Ren L. Simulation Analysis of Impulsive Ankle Push-Off on the Walking Speed of a Planar Biped Robot. Front Bioeng Biotechnol 2021;8:621560. DOI: 10.3389/FBIOE.2020.621560
32. Hausdorff JM. Gait dynamics in Parkinson's disease: Common and distinct behavior among stride length, gait variability, and fractal-like scaling. Chaos 2009;19:026113. DOI: 10.1063/1.3147408
33. Salazar-Varas R, Costa A, Úbeda A, Iáñez E, Azorín JM. Changes in brain activity due to the sudden apparition of an obstacle during gait. International IEEE/EMBS Conference on Neural Engineering, NER 2015;2015-July:110–3. DOI: 10.1109/NER.2015.7146572
34. Azizi T. On the fractal geometry of gait dynamics in different neuro-degenerative diseases. Physics in Medicine 2022. DOI: 10.1016/j.phmed.2022.100050

نشریه فناوری ورزشی پیشرفته
DOI: 10.22098/jast.2025.18618.1444
تاریخ دریافت: ۱۴۰۳/۱۱/۱۸ تاریخ پذیرش: ۱۴۰۴/۲/۲۹
Journal of Advanced Sport Technology
«مقاله پژوهشی»

تحلیل پیچیدگی چندفرکتالی سیگنال‌های EEG و دینامیک کینماتیکی در راه رفتن

روح الله بساط نیا [۱]، مهرداد عنبریان *[۲]، افشین منتخب [۳]

۱. دانشجوی دکتری، گروه بیومکانیک ورزشی، دانشکده علوم ورزشی، دانشگاه بوعلی سینا، همدان، ایران.
۲- استاد بیومکانیک ورزشی، گروه بیومکانیک ورزشی، دانشکده علوم ورزشی، دانشگاه بوعلی سینا، همدان، ایران.
۳- گروه فیزیک، دانشکده فیزیک، دانشگاه شیراز، شیراز، ایران.

نویسنده مسئول: مهرداد عنبریان/ m.anbarrian@basu.ac.ir

چکیده

زمینه :راه رفتن، به عنوان یک فعالیت حرکتی پیچیده، نیازمند هماهنگی دقیق در سیستم عصبی–عضلانی است. این مطالعه با هدف تحلیل پیچیدگی چندمقیاسی سیگنال‌های الکتروانسفالوگرافی (EEG) و داده‌های کینماتیکی در فرآیند راه رفتن انجام شد تا تعاملات مغز و اندام تحتانی حین راه رفتن بررسی شود.

روش‌ها :سیزده آزمودنی مذکر روی تردمیل در شرایط کنترل‌شده راه رفتند، که طی آن سیگنال‌های EEG و داده‌های کینماتیکی ثبت شدند. تحلیل پیچیدگی چندفرکتالی با استفاده از روش تحلیل نوسانات دترندشده چندفرکتالی (MF-DFA) بر روی داده‌ها اعمال شد تا نمای هرست به عنوان شاخص پیچیدگی برای ویژگی‌های دینامیکی حرکات در ابعاد جابه‌جایی در سه محور(X ، Y، Zو فعالیت قشری در نواحی حرکتی مغز C3) و (C4 حین راه رفتن استخراج گردد.

نتایج :نتایج نشان داد که نمای هرست تعمیم‌یافته H(q) در نواحی C3 و C4 مشابه است و همبستگی مثبت معنی‌داری با همان پارامتر در دینامیک اندام مقابل نشان می‌دهد، که از اصل کنترل متقابل نیمکره‌ای حمایت می‌کند. تحلیل سگمنتال ران، ساق و پا تقارن دینامیکی قابل توجهی بین سمت راست و چپ را آشکار ساخت. الگوهای چندفرکتالی سگمنت‌ها تفاوت معنی‌داری را نشان داد، با بالاترین H(q) در ساق و پایین‌ترین در ران. هماهنگی درون‌سیستمی قوی بین سگمنت‌ها نشان‌دهنده سازماندهی یکپارچه در کنترل حرکتی است.

نتیجه‌گیری :این یافته‌ها تقارن و هماهنگی عصبی–عضلانی را تأیید می‌کنند، برای ارزیابی اختلالات حرکتی و طراحی پروتکل‌های توانبخشی مفید هستند و بر اهمیت تحلیل چندمقیاسی در روشن‌سازی تعاملات پیچیده مغز–بدن تأکید دارند، با کاربردهای بالقوه در تحقیقات علوم اعصاب، بیومکانیک و توانبخشی.

واژه‌های کلیدی: **راه رفتن، سیگنال‌های EEG، داده‌های کینماتیکی، تحلیل چندفرکتالی، نمای هرست**